Understanding London's summertime cloud cover

Theeuwes, N. E. ORCID: https://orcid.org/0000-0002-9277-8551, Boutle, I. A., Clark, P. A. ORCID: https://orcid.org/0000-0003-1001-9226 and Grimmond, S. ORCID: https://orcid.org/0000-0002-3166-9415 (2022) Understanding London's summertime cloud cover. Quarterly Journal of the Royal Meteorological Society, 148 (742). pp. 454-465. ISSN 1477-870X doi: https://doi.org/10.1002/qj.4214 Available at https://centaur.reading.ac.uk/101357/

Received: 14 May 2021 | Revised: 3 October 2021 | Accepted: 10 November 2021

DOI: 10.1002/qj.4214

Quarterly Journal of the Royal Meteorological Society RMetS

RESEARCH ARTICLE

Understanding London's summertime cloud cover

Natalie E. Theeuwes[1,2] | **Ian A. Boutle**[3] | **Peter A. Clark**[1] | **Sue Grimmond**[1]

[1]Department of Meteorology, University of Reading, Reading, UK

[2]Royal Netherlands Meteorological Institute, De Bilt, The Netherlands

[3]Met Office, Exeter, UK

Correspondence
N. E. Theeuwes, Royal Netherlands Meteorological Institute, De Bilt, The Netherlands
Email: natalie.theeuwes@knmi.nl

Funding information
NWO Rubicon grant 'Clouds above the city' (019.161LW.02), The UK–China Research & Innovation Partnership Fund through the Met Office Climate Science for Service Partnership (CSSP) as part of the Newton Fund, EPSRC Data Assimilation for the REsilient Cities (DARE), NERC Climate service for resilience to overheating risk in Colombo, Sri Lanka: a multi-scale mapping approach (COSMA)

Abstract

Cities are a source of complex land–atmosphere interactions. Spatial differences in the energy balance and enhanced surface roughness interact with the atmosphere to alter clouds and precipitation. Here, we explore how London (UK) alters cloud formation during the spring and summer. The Met Office's high-resolution operational forecasts predict enhanced cloud cover over the city, as found in observations, but underpredicts the intensity. During low wind speeds, cloud enhancement over the city is strongest and linked to an urban-induced thermal circulation. These circulations advect moist air from the city edge inwards, transporting it upwards with a large moisture convergence over the urban area. At around 1,000 m above the surface, the turbulent moisture flux takes over the moisture transport to the cloud layer. A relative humidity budget shows the moisture flux in the upper boundary layer to be the largest contribution to the urban–rural differences in relative humidity.

KEYWORDS

atmospheric boundary layer, clouds, moisture transport, urban

1 | INTRODUCTION

Urban areas are known to impact local weather and climate, including temperature and precipitation. This is a result of the distinctly different surface properties of cities compared to their rural surroundings. Urban areas generally have a different energy-balance partitioning compared to rural areas (e.g., Grimmond and Oke, 1995; Christen and Vogt, 2004), which leads to the spatial temperature difference, known as the urban heat island (UHI). Stored heat released from building fabric, plus anthropogenic sources of heat, slow the cooling of the surface in the evening transition and temperatures in cities remain higher than their rural surroundings. In addition, the complex urban surface (e.g., buildings) changes the overall roughness of the surface, leading to changes in turbulence and city-scale wind speed patterns (e.g., Bornstein and Johnson, 1977; Roth, 2000; Drew *et al.*, 2013).

Several studies have found cities to impact precipitation, generally increasing rainfall amounts over and downwind of urban areas (Changnon *et al.*, 1971; Liu and Niyogi, 2019; Li *et al.*, 2020). A long-term observational study in the United States showed the amount of precipitation enhancement is dependent on the size of the urban area (Kingfield *et al.*, 2018). Dou *et al.* (2015) found rainfall patterns in the Beijing area varied based on the strength of the urban heat island, with precipitation enhancement over and downwind of the city during strong UHI, and storm bifurcation during weak UHI events.

Three processes are hypothesised to impact urban-influenced convection. First, differences in the energy-balance partitioning. In temperate climates, with generally less vegetation in cities, less energy is partitioned into latent heat flux, but more into both the storage and sensible heat fluxes. This leads to higher boundary-layer heights over the urban area (e.g., Barlow *et al.*, 2015) and a higher lifting condensation level (e.g., Theeuwes *et al.*, 2019). Whether the combined effect leads to an increase in cloud formation depends on stability of the atmosphere above the boundary layer, the convective triggering potential (Findell and Eltahir, 2003a). In addition, the spatial variability in the energy-balance partitioning could lead to thermally driven circulations during low wind speed conditions (e.g., Lemonsu and Masson, 2002; Han and Baik, 2008; Wang, 2009; Varentsov *et al.*, 2018). This circulation can cause large updraughts over the city triggering convection, and can add to the transport of moisture from outside the city (e.g., Han and Baik, 2008; Zhu *et al.*, 2017). Second, the enhanced surface roughness could cause frictional convergence over the city (e.g., Thielen *et al.*, 2000; Rozoff *et al.*, 2003). Third, urban areas are sources of air pollution, with some of the released aerosols acting as cloud condensation nuclei, which could alter precipitation in the vicinity of cities (Schmid and Niyogi, 2017).

It is important to forecast large convective systems near urban areas accurately as they have diverse consequences for the large population living within them. However, the Liu and Niyogi (2019) literature review finds that modelling studies underestimate the impact of the urban surface on precipitation enhancement compared to observational studies. It is unclear if this is caused by model resolution or missing processes. To understand how urban areas influence land–atmosphere interactions leading to convection, this study steps back and analyses the influence of cities on low or boundary-layer clouds.

The very few studies that have analysed the influence of urban areas on cloud formation mostly use observations (e.g., Angevine *et al.*, 2003; Theeuwes *et al.*, 2019). Both these studies find an increase in the cloud-base height over the urban area, related to the drier subcloud layer. Theeuwes *et al.* (2019) found an increase in cloud cover during the afternoon and evening transition over London, UK and Paris, France, coinciding with longer-lasting buoyancy-driven turbulence. The aim of this study is to investigate whether a state-of-the-art high-resolution numerical weather prediction model is able to reproduce the enhancement of cloud cover over the mega city, London. Forecasts from the UK Met Office's limited-area operational model (UKV) are analysed and evaluated for spring and summer months of one year, where sufficient observations for evaluation are available and urban–cloud interactions are shown to be strong (Theeuwes *et al.*, 2019). Analysing an entire season allows us to move beyond case-studies and study the driving mechanisms responsible for the summertime cloud cover enhancement over the city.

2 | UKV FORECASTS

Met Office UKV operational forecasts have a limited-area configuration with 70 quadratically spaced vertical levels below 40 km and a horizontal grid spacing of 1.5 km over the UK, increasing to 4 km at the boundaries (Figure 1). They are one-way nested inside the Met Office operational global model (Walters *et al.*, 2017), and both are configurations of the Unified Model. Although the forecast runs every 3 hr using a 3D-Var data assimilation system, we analyse the 2100 UTC forecasts. The science configuration of the UKV is the same as that detailed in Boutle *et al.* (2016).

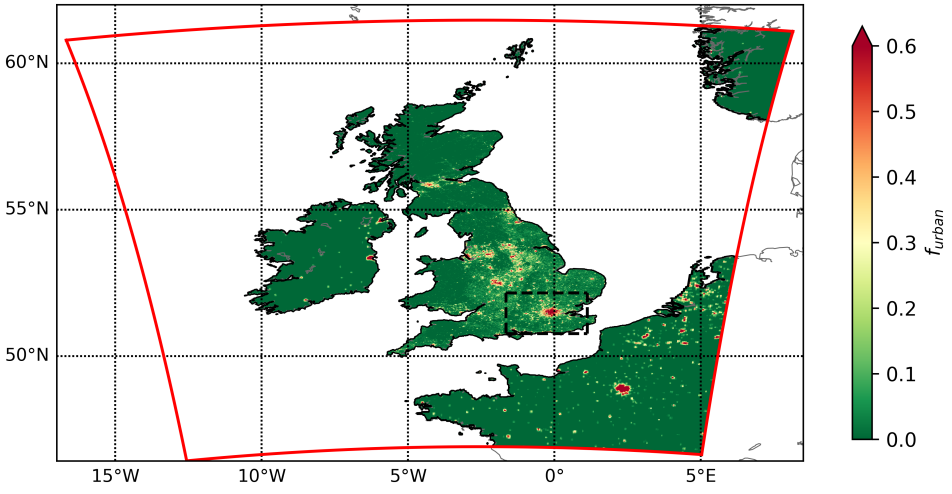

FIGURE 1 Spatial extent of the domain of the UKV forecasts (solid lines) and the impervious ('urban') fraction used in the model domain (colour shading). The black dashed box is the study area [Colour figure can be viewed at wileyonlinelibrary.com]

The land–surface exchanges are parametrized using JULES (Joint UK Land Environment Simulator; Best *et al.*, 2011), with nine tiles to represent five vegetated and four non-vegetated surfaces. The single-tile urban scheme of Best (2005) represents both the enhanced surface roughness and reduced latent heat flux expected in an urban area. Atmospheric turbulence is parametrized following Lock *et al.* (2000) and Brown *et al.* (2008) for vertical mixing, including non-local fluxes of heat and momentum. Horizontal mixing is parametrized with a 2D Smagorinsky scheme. The diagnostic cloud scheme follows Smith (1990), with a height-varying profile of critical relative humidity. The conversion of cloud water into rain is dependent on the cloud droplet number concentration (Wilkinson *et al.*, 2013), which in turn is calculated from a single-species prognostic aerosol (Clark *et al.*, 2008). Therefore the model also represents enhanced pollution over urban areas and the effect this may have on precipitation.

The study period 1 May to 31 August 2014 was selected due to the simultaneous observations available at both rural and urban sites (Section 3.1). Additionally, in later analysis the focus is on understanding the processed leading to cloud enhancement over London during low wind speed conditions (Sections 5–7). The spring and summer season of 2014 had a relatively large amount of cases with these low wind speed conditions (31.6% compared to an average ∼23% between 2013 and 2016), and thus provided a large number of cases for analysis of the processes.

3 | OBSERVATIONS

3.1 | Surface-based observations

The model forecasts are evaluated using several datasets, at urban and rural locations. The rural location, Chilbolton (51°09′N, 01°26′W), used in previous model evaluation studies (e.g., Illingworth *et al.*, 2007; Hogan *et al.*, 2009) has 30 min sensible and latent heat fluxes derived from a Metek USA-1 sonic anemometer with a LiCOR Li-7500 open-path gas analyser measuring at 20 Hz, at 5.3 m above ground level (agl). Fluxes at the closest grid points in model output are used in the evaluation from 25 July 2014 onward. Temperature and relative humidity measured at 1.5 m using a Vaisala HMP155A. Cloud base and occurrence are determined from a Vaisala CT75K ceilometer which measures at 30 s temporal and 30 m vertical resolution.

In London, measurements are at two locations. An eddy covariance system mounted on a triangular tower on the roof at King's College London (KCL, 51°30′43.3″N, 0°06′58.6″W), 50.3 m agl, making it ∼2.2 times the mean building height (Kotthaus and Grimmond, 2014). A Campbell Scientific CSAT3 sonic anemometer combined with a LiCOR Li-7500A open-path gas analyser measuring at 10 Hz to give 30-min fluxes (Kotthaus and Grimmond, 2014). Latent heat fluxes are available until 28 June 2014. London's cloud base and occurrence are measured with a Vaisala CL 31 ceilometer located at Marylebone Road (51°31′21.1″N, 0°09′16.5″W) with a vertical resolution of 10 m and temporal resolution of 15 s.

Ceilometer cloud-base heights are resampled to 15 min, allowing a larger proportion of the sky to be studied. The fifth percentile of cloud-base height for each 15-min interval (Kotthaus and Grimmond, 2018) is analysed indicating the cloud-base height over a few kilometres, depending on wind speed. The fifth percentile is used as a minimum cloud-base height, excluding occasional outliers. Both ceilometers operate at the 905 μm wavelength.

3.2 | Satellite data

Cloud cover is calculated from MSG-SEVIRI High Resolution Visible (HRV) broadband channel (0.4–1.1 μm) images following the methodology of previous studies (Teuling *et al.*, 2017; Theeuwes *et al.*, 2019). A cloud mask for May, June, July, and August is created per pixel for hourly intervals each 10-day period to reduce seasonal and diurnal variability in surface albedo and solar zenith angle. Ten years of data (2010–2019) are used to derive the cloud thresholds. The 400 HRV radiation values per pixel (10 years × 10 days × 4 per hour) are sorted and the cumulative frequency distribution (CFD) determined. Spikes are removed using a triangular moving-average smoothing. The maximum gradient in the CFD is defined to be the cloud threshold for this pixel. The cloud mask is created by assuming every HRV radiation value above this cloud threshold to be cloudy and anything below the threshold is defined to be clear. The cloud masks are used to calculate temporally averaged cloud cover. Short periods (1 hr, 10 days) when cloud thresholds are calculated will limit the effect that occasionally mis-classified pixels have on the overall temporally averaged cloud cover.

4 | MODEL EVALUATION

4.1 | Surface variables

Before assessing the ability of the forecast to predict cloud cover, (near-)surface variables important for cloud formation are assessed. Figure 2a, b show the turbulent surface fluxes for the urban and rural site. At Chilbolton

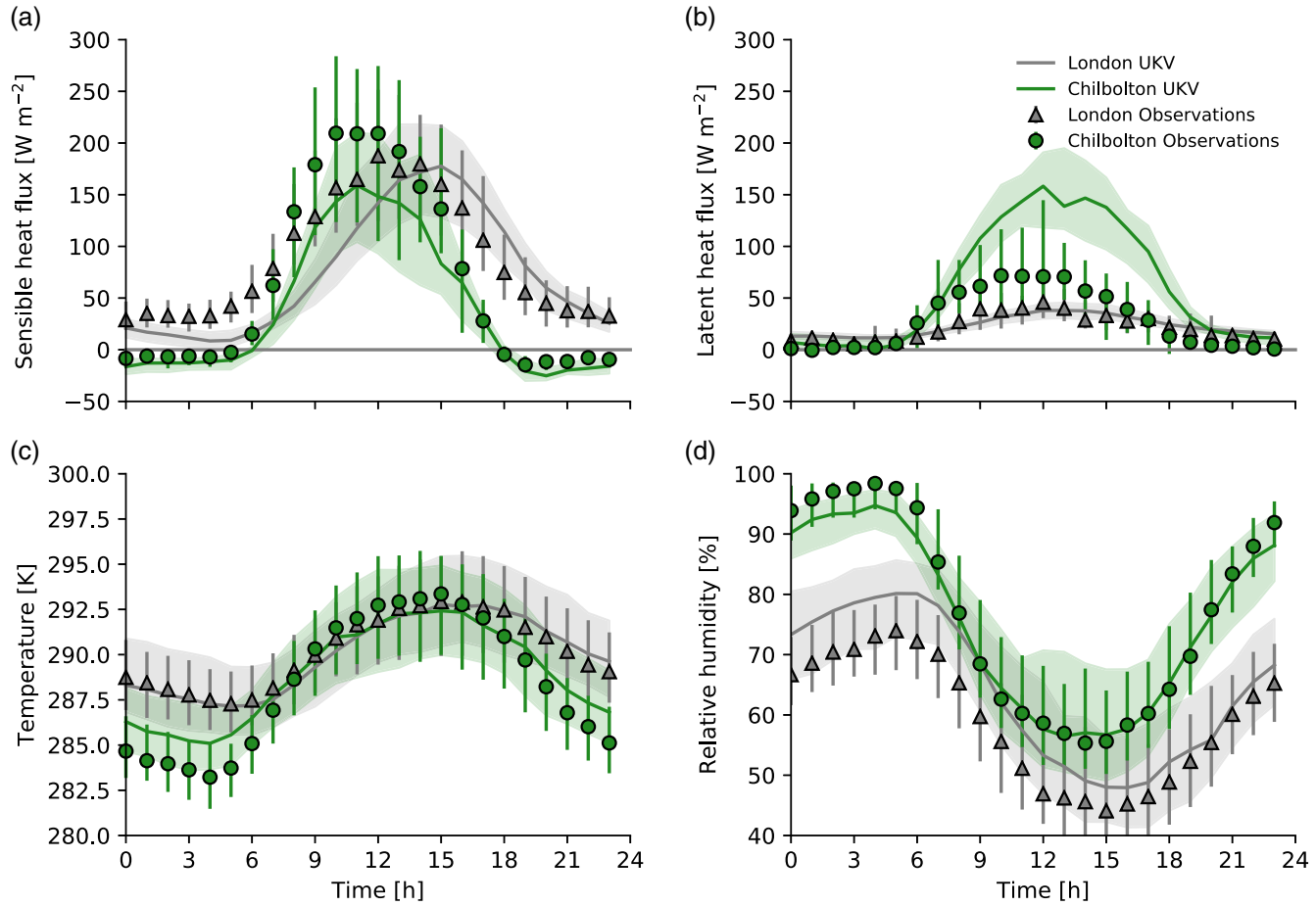

FIGURE 2 Modelled and observed median diurnal cycle (lines, points) with interquartile ranges (shading, vertical lines) for London and Chilbolton of: turbulent (a) sensible heat flux (with $n_{\text{London}} = 102$ and $n_{\text{Chilbolton}} = 39$) and (b) latent heat flux (with $n_{\text{London}} = 55$ and $n_{\text{Chilbolton}} = 39$), and near-surface (c) absolute temperature ($n = 106$) and (d) relative humidity ($n = 106$), where n indicates the number of days available for analysis. Observations from the London KCL site (dots) and Chilbolton (triangles) are plotted with the corresponding UKV forecasts for 3 × 3 grid cells (lines). The study period runs from 1 May 2014 to 31 August [Colour figure can be viewed at wileyonlinelibrary.com]

the forecasts generally underestimate the Bowen ratio, as the latent heat flux is overpredicted (mean absolute error (MAE) 53.6 W·m^{-2} and median bias (MB) 18.0 W·m^{-2}) and the sensible heat flux is underpredicted (MAE 33.7 W·m^{-2}, MB –10.5 W·m^{-2}). In the 3 × 3 grid area analysed, the surface is classified as C3 grass (0.74), bare soil (0.18), and trees (0.08).

Compared to the turbulent surface fluxes at Chilbolton, the sensible and latent heat fluxes in central London are well-predicted. The latent heat flux is small, which is the result of minimal vegetation (C3 grass 0.11) but extensive impervious (0.78 buildings and paved) area, and therefore reduced evaporation. Also in the 3×3 model grid cells around the measurement site is water (0.07) and bare soil (0.04). The model predicts the magnitude of the sensible heat flux well, however the increase in the morning flux is delayed, consistent with the results of Warren *et al.* (2018). This phase lag is a result of the urban scheme used. During the 2014 forecasts, JULES used the Best one-tile scheme (Best, 2005) which added an urban canopy tile which was radiatively coupled to the soil and used a high areal heat capacity (0.28 J·K^{-1} · m^{-2}). This approach results in a shift of the sensible heat flux towards the evening transition (Hertwig *et al.*, 2020), enabling the night-time urban temperatures to be reproduced well (Figure 2c).

The near-surface temperature and relative humidity are modelled accurately during the daytime, especially over the rural site (Figure 2c, d). Although the latent heat flux over Chilbolton is overestimated, the relative humidity is modelled well with a slight underestimation during the night (root mean squared error (RMSE) 7.43%, MAE 5.26%, MB −1.28%). However, the RMSE, MAE, and MB for air temperature at Chilbolton are 1.58, 1.25, and 0.57 K, respectively. Especially during the night, the Chilbolton air temperature is high. Combined with the underestimation of the Bowen ratio, this could point to an overestimation

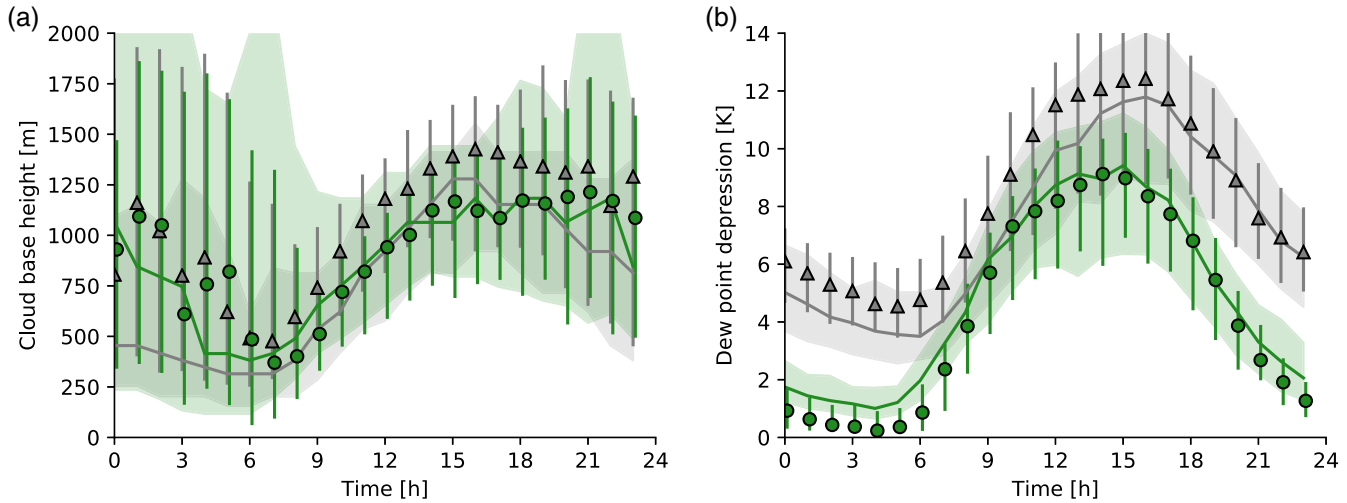

FIGURE 3 As Figure 2, but for (a) cloud-base height below 3 km above the surface ($n_{\text{London}} = 69$ to 116 and $n_{\text{Chilbolton}} = 67$ to 114) and (b) dew point depression ($T - T_{\text{d}}$) ($n = 106$) for all data from May to August 2014 [Colour figure can be viewed at wileyonlinelibrary.com]

of the soil moisture in the UKV forecasts for this period. At the London site the near-surface temperature is predicted very well (RMSE 1.01 K, MAE 0.73 K, MB −0.19 K). There is a slight underestimation in the morning transition, related to the delayed increase of the morning sensible heat flux (Figure 2a). However, at the London site the modelled air is not dry enough; the relative humidity is overpredicted (RMSE 8.60%, MAE 6.76%, and MB 4.59%).

4.2 | Clouds

Overestimation of the relative humidity in central London is consistent with cloud-base height forecast skill (Figure 3a). Day-time dew point depression, an indicator for the daytime lifting condensation level (Lawrence, 2005), is forecast to be smaller than observed, with a daytime MB −0.98 K (i.e., the dew-point is closer to the air temperature in the forecast) (Figure 3b). We consider this underestimation to be predominantly caused by the overestimation of the dew-point temperature (since the temperature is well-predicted, Figure 2c). The moister sub-cloud layer leads to an underestimation of the cloud-base height, with a daytime MB −161.9 m (Figure 3b). As a result, the large difference in cloud-base heights found in observational studies (e.g., Angevine *et al.*, 2003; Theeuwes *et al.*, 2019) is underestimated in the UKV forecasts.

Generally, the UKV forecasts underestimate the spatial variability in cloud cover compared to the observations (Figure 4), although it correctly predicts an enhancement of cloud cover over the urban area. The ceilometer-observed difference in cloud occurrence between the two sites (London and Chilbolton) varies from 9% at 1200 UTC to a maximum of 16% at 2100 UTC (Figure 4a), while the UKV forecast difference between these two sites varies between 1% at 1200 UTC and 11% at 2200 UTC.

Satellite images permit a spatial comparison. As the MSG-HRV channel is in the visible spectrum, only daytime model evaluation is possible. Henceforth, we focus on the afternoon when the model performs best (cf. observations) for the (near-)surface variables. The afternoon is also when the strongest cloud enhancement is present during the daylight hours.

Seasonally averaged, the model predicts both the spatial patterns of cloud cover and the higher cloud occurrence over urban London. Between the coast and northwest of London, the modelled gradient in cloud cover is smaller than the satellite data indicate (Figure 4b, d). The satellite data show the area east of the urban measurement site (Figure 4 grey triangle) has 15% higher cloud cover than the domain-averaged cloud cover. The UKV forecasts rightly predict the city's cloud-cover maximum to occur to the east of this site, but with an 8% higher cloud cover than the domain average.

The enhanced cloud cover over London in the model can be related to several mechanisms. The higher sensible heat flux (cf. rural surroundings) can lead to a higher boundary-layer height, with a lifted parcel having longer to condense, consistent with what is seen over dry soils (Findell and Eltahir, 2003b; Westra *et al.*, 2012). Larger sensible heat fluxes can also cause the thermally driven circulation known as the urban breeze (Lemonsu and Masson, 2002; Hidalgo *et al.*, 2008). This circulation causes convergence over the city, leading to horizontal transport of moisture and convection. In addition, the higher roughness length

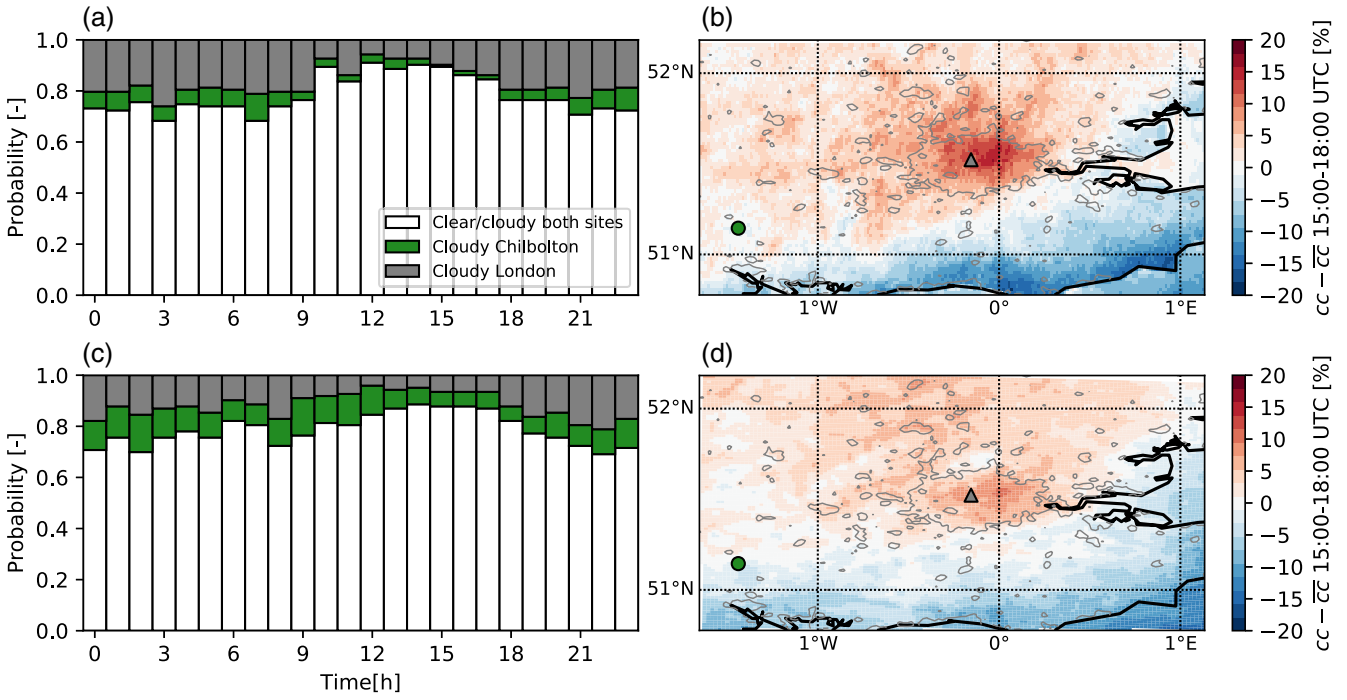

FIGURE 4 Observed and modelled cloud cover. (a, c) Probability of simultaneously observed clouds or clear sky over London Marylebone Road and Chilbolton and cloud observed only over London or Chilbolton determined from (a) ceilometers and (c) UKV forecasts. (b, d) Spatial extend of the afternoon averaged cloud cover deviation (cloud cover at each grid cell (cc) minus domain-averaged cloud cover ($\overline{cc}$)) determined from (b) satellite data and (d) forecast cloud cover. Urban areas (impervious fraction > 0.2) are indicated by grey lines. Data are from May to August 2014 ($n = 123$) [Colour figure can be viewed at wileyonlinelibrary.com]

over the urban area could cause frictional convergence over the city. Thermally driven circulations are often found when background wind speeds are below 3–4 $m \cdot s^{-1}$ (e.g., Varentsov *et al.*, 2018), whereas frictional convergence only starts to dominate under strong wind speeds. Between these, both processes may play a role (Omidvar *et al.*, 2020). Therefore, we stratify the forecasts into three categories based on the wind speed above the roughness sublayer at 70 m: low ($\overline{U} < 4\ m \cdot s^{-1}$), medium ($4 < \overline{U} < 8\ m \cdot s^{-1}$), and high ($\overline{U} > 8\ m \cdot s^{-1}$) wind speeds which occurred 31.6%, 47.2%, and 21.1% of the time, respectively, in the May to August 2014 period.

In all three wind regimes, the satellite data have higher cloud cover over London (cf. domain average, Figure 5). This difference is largest for low wind speeds, with $cc - \overline{cc}$ up to 20% over the centre of London. Satellite observations during low wind speed conditions also show enhanced cloud cover over the forested area southwest of London, consistent with forested areas in France (Teuling *et al.*, 2017; Bosman *et al.*, 2019). However, the UKV forecasts do not reproduce this enhancement.

Under the low and medium wind speed conditions, enhanced cloud cover over London is forecast by the UKV, but the absolute cloud cover differences (urban area cf. domain average) are approximately 6–8% lower than observed. These cases forecast a similar cloud cover magnitude associated with orography north and northwest of the city. Despite this overprediction of orography-associated convection, henceforth we focus on low wind speed conditions where the cloud enhancement over the urban area is strongest and closely represents the observations – 39 days in total.

5 | MOISTURE TRANSPORT

The west–east cross-section for low wind speed cases in 2014 shows an enhancement of the liquid water mixing ratio over London, with an average up to 0.07 $g \cdot kg^{-1}$ (Figure 6a). The maximum coincides with large updraughts over the region with the highest urban fraction, $w > 0.060\ m \cdot s^{-1}$. East of the urban area there are descending motions with an average vertical velocity of $< -0.030\ m \cdot s^{-1}$. Therefore, during the afternoon, the higher buoyancy flux combined with the sea-breeze to the east of the city creates a thermal circulation. The frequency of the sea-breeze is sufficient to be present in the average. This circulation causes convergence over the city (Figure 6c). Previous research found the interaction between an urban-induced thermal circulation and sea-breeze circulation could enhance updraughts over the city (e.g., Ado, 1992).

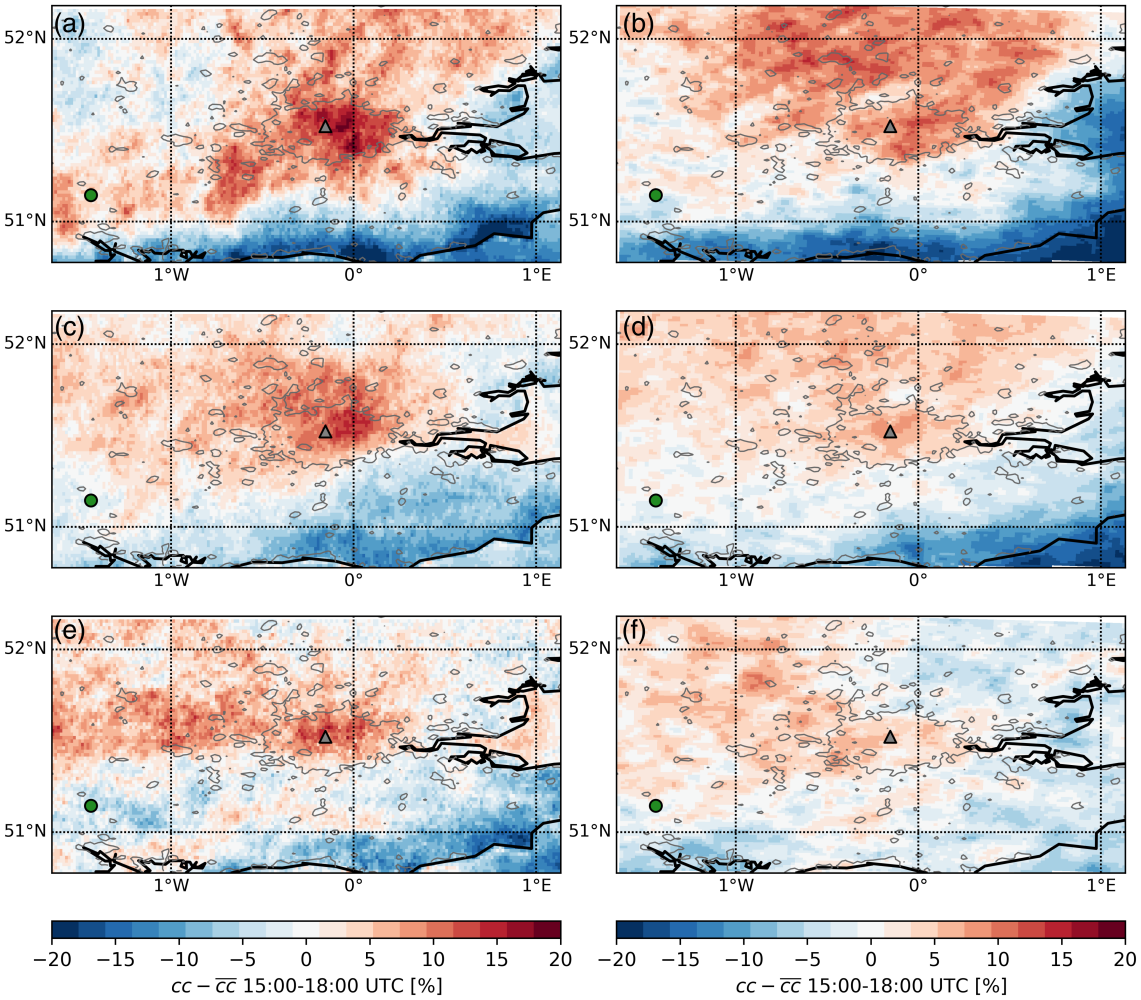

FIGURE 5 Spatial extent of the afternoon averaged cloud cover deviation (cloud cover at each grid cell (cc) minus domain-averaged cloud cover ($\overline{cc}$), determined from (a, c, e) satellite and (b, d, f) forecast cloud cover. Data are stratified by domain-averaged 70 m wind speeds: (a,b) $< 4\,\mathrm{m{\cdot}s^{-1}}$ ($n = 39$), (c, d) between 4 and $8\,\mathrm{m{\cdot}s^{-1}}$ ($n = 58$), and (e, f) $> 8\,\mathrm{m{\cdot}s^{-1}}$ ($n = 26$). [Colour figure can be viewed at wileyonlinelibrary.com]

In the lowest 300 m of the atmosphere, the thermal circulation causes moist air from the edges of the city to be advected into the city (Figure 6b). Consequently, there is a high moisture convergence over the eastern half of London, transporting the moisture upward (Figure 6c), with divergence starting around 1,500 m. Moisture is also advected from the sea westwards very close to the surface, but is not advected into the urban area. The horizontal advection upwind of London is also small. Therefore we assume most of the moisture originates near the edges of the city, where the latent heat flux is still large given the higher vegetation fractions. Using idealised large-eddy simulation of convection over heterogeneous surfaces, several studies have shown a similar transport of moisture from surfaces of lower to higher Bowen ratio (van Heerwaarden *et al.*, 2008; Zhu *et al.*, 2017).

The near-surface vertical moisture flux is large (averages $\sim 0.055\,\mathrm{g{\cdot}kg^{-1}m{\cdot}s^{-1}}$) above the rural surface (Figure 6d), but much lower over more impervious areas, where the mean for the centre of London is $0.014\,\mathrm{g{\cdot}kg^{-1}{\cdot}m{\cdot}s^{-1}}$. However, in the upper part of the boundary layer, the vertical moisture flux is higher over the urban area than over the surrounding rural areas. At around 1,000 m agl, the moisture transported upwards by convergence is transported to the cloud layer with the vertical turbulent moisture flux. At the edge of the city ($x \approx 110$ km, Figure 6), the moisture flux is about $0.008\,\mathrm{g{\cdot}kg^{-1}{\cdot}m{\cdot}s^{-1}}$ higher than the rural area west of London. This could indicate that part of the advected moisture is transported upwards at the edge of the urban area.

6 | RELATIVE HUMIDITY BUDGET

Whether an air parcel condenses to form a cloud depends on the relative humidity (RH). The relative humidity is

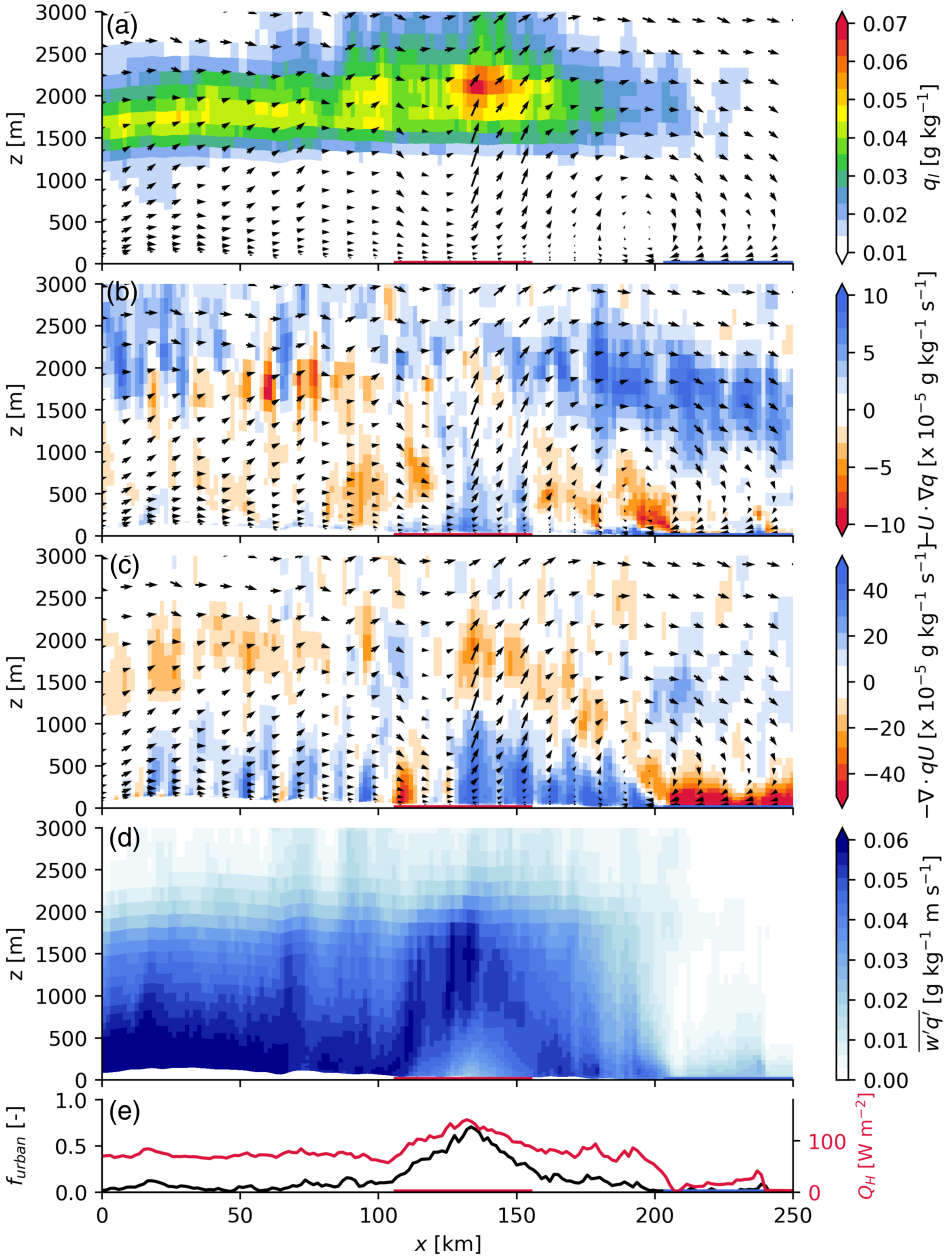

FIGURE 6 West–east cross-section of the average (a) liquid water mixing ratio, (b) sum of all horizontal moisture advection terms, (c) moisture convergence (positive) and divergence (negative), (d) vertical moisture flux, and (e) urban surface fraction (black) and surface sensible heat flux (red) for low (<4 m·s^{-1}) wind speeds between 1400 and 1800 UTC, from 2100 UTC forecasts in May to August 2014) (n = 39). Cross-sections are averaged over a 30 km north–south band. Extents of London (red line) and sea (blue line) are shown on the lower axis [Colour figure can be viewed at wileyonlinelibrary.com]

impacted by both the amount of moisture in the atmosphere and the temperature. To assess if the enhanced liquid water for the low wind speed cases is associated with the moisture or temperature contribution, we separate the moisture and temperature (T) terms in the relative humidity budget (Ek and Mahrt, 1994):

$$\frac{\partial RH}{\partial t} = \underbrace{\frac{1}{q_s}\frac{\partial q}{\partial t}}_{q-\text{term}} - \underbrace{\frac{RH}{q_s}\frac{\mathrm{D}q_s}{\mathrm{D}T}\frac{\partial T}{\partial t}}_{T-\text{term}}, \quad (1)$$

where q_s is the saturation specific humidity and q specific humidity. Here, $\mathrm{D}q_s/\mathrm{D}T$ is the slope of the saturation specific humidity versus temperature curve.

The change in specific humidity can be expressed as:

$$\frac{\partial q}{\partial t} = -u\frac{\partial q}{\partial x} - v\frac{\partial q}{\partial y} - w\frac{\partial q}{\partial z} - \frac{\partial \overline{u'q'}}{\partial x} - \frac{\partial \overline{v'q'}}{\partial y} - \frac{\partial \overline{w'q'}}{\partial z}, \quad (2)$$

and absolute temperature:

$$\frac{\partial T}{\partial t} = -u\frac{\partial T}{\partial x} - v\frac{\partial T}{\partial y} - w\frac{\partial T}{\partial z} - \frac{\partial \overline{u'T'}}{\partial x} - \frac{\partial \overline{v'T'}}{\partial y} - \frac{\partial \overline{w'T'}}{\partial z}. \quad (3)$$

Here, the first three terms on the right-hand side are the horizontal and vertical advection terms, and the last three are the turbulent transport terms. In these forecasts the vertical turbulent transport is parametrized using the

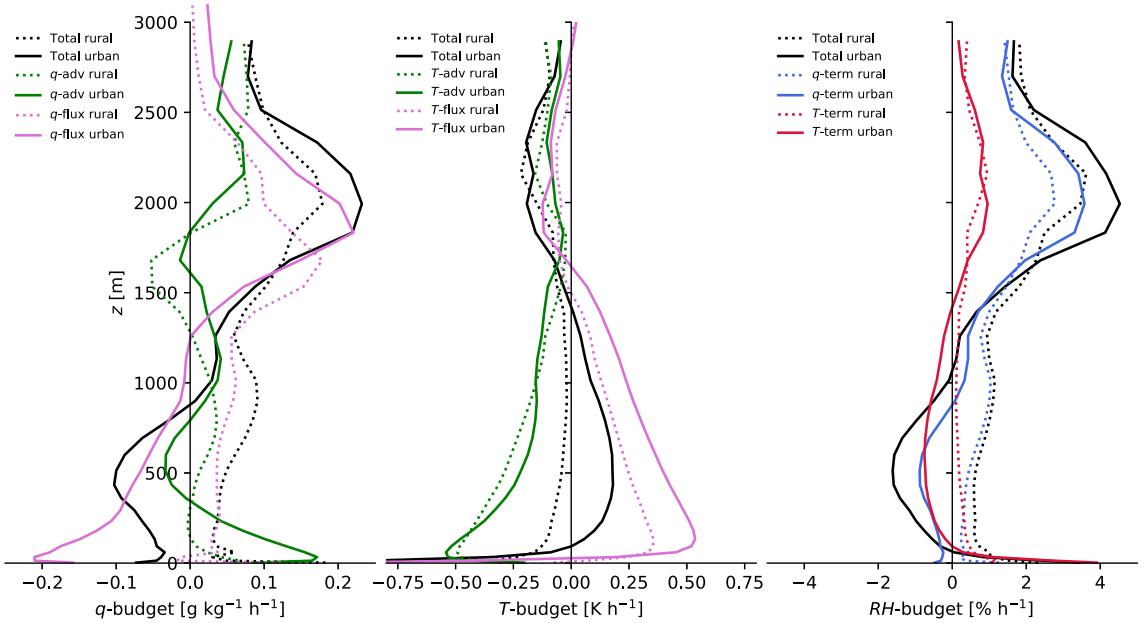

FIGURE 7 May to August 2014 domain-averaged vertical profiles during low (<4 m·s^{-1}) wind speeds of (a) specific humidity (b) absolute temperature, both split into flux components, advection components, and (c) relative humidity budgets, split into contributions from temperature and moisture and the total. Averages are for two 30 km areas: rural (dashed lines, 40 km west of London), and urban (solid lines, in London) (n = 39) [Colour figure can be viewed at wileyonlinelibrary.com]

1D Lock *et al.* (2000) scheme and the horizontal turbulent transport is small.

In Figure 7 the vertical profile of each term is plotted for two 900 km^2 areas, one inside London and the other west (upwind) of London, for all the low wind speed cases. The total moisture transport is lower in the sub-cloud layer over London, caused by the difference in the flux component being larger than the advection term. However, above 1,500 m there is a larger moisture term in the urban column. The majority of this additional moisture aloft comes from the turbulent flux (Figure 6d). Close to the surface the urban and rural columns have a large difference in the moisture advection term. The horizontal gradient of moisture (i.e., drier urban surface layer) results in moisture being advected within the urban area itself, from the edge of the city in the lowest 300 m (as noted in Section 5, Figure 6b).

The mean changes in temperature are small around the cloud layer, but larger in the sub-cloud layer (Figure 7b). The lower part of the urban boundary layer is heated more than the slightly cooled rural column. This urban heating is from the additional surface sensible heat flux (cf. rural) at the surface (urban = 124 versus rural = 74 W·m^{-2}). In both the urban and rural columns there is negative temperature advection of similar magnitude.

For the relative humidity budget, in the urban sub-cloud layer there is a net decrease in relative humidity from the heating and drying in the lower boundary layer (Figure 7c). The rural sub-cloud layer relative humidity increases with the cooling and moistening of this layer. However, above 1,000 m the net relative humidity increases. Above 1,500 m in the cloud layer the increase in relative humidity in the urban column is greater than in the rural column. This increased relative humidity in the cloud layer is directly related to the increase in moisture from the higher turbulent moisture transport.

7 | DISCUSSION

The model simulations consider aerosol–cloud interactions, but only the second indirect effect. The Tripoli and Cotton (1980) auto-conversion scheme is activated by a threshold value of cloud liquid water and used to convert cloud water into rain. Both the threshold value and conversion rate are dependent on the cloud droplet number concentration (Wilkinson *et al.*, 2013), which is calculated from a single-species prognostic aerosol within the model (Clark *et al.*, 2008).

Small aerosol concentrations outside the city may possibly cause clouds to rain out, whereas above the city enhanced aerosols may suppress precipitation, increasing cloud lifetime. To exclude this effect, the analysis is repeated excluding all cases with rain within 45 km around London. This decreases the number of cases from 39 (Figure 6) to 27 (Figure 8). The mechanisms (discussed in Sections 5 and 6) do not change markedly when stratiform rain cases are excluded. There is still an enhancement of

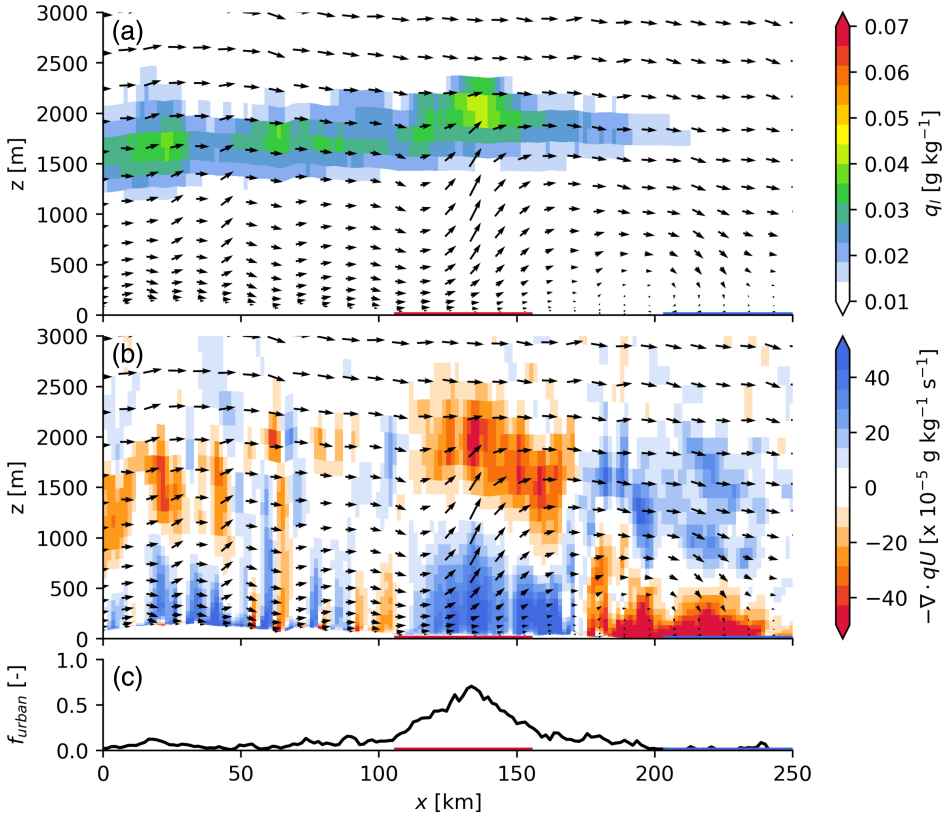

FIGURE 8 As Figure 6a, c, e, but for low (<4 m·s^{-1}) wind speeds where stratiform rain = 0 kg·m^{-2}·s^{-1} from 45 km west of the edge of London to the coast east of London (n = 27) [Colour figure can be viewed at wileyonlinelibrary.com]

liquid water over the urban surface (Figure 8a), caused by a thermal circulation, resulting in moisture convergence over London and divergence aloft (Figure 8b). Therefore, in these low wind speed conditions, aerosol–cloud interactions play a small role in creating the modelled urban-enhanced cloud cover in the UKV forecasts. While some studies have found some suppression of precipitation (e.g., Rosenfeld, 2000; Zhong *et al.*, 2015; Schmid and Niyogi, 2017), more research is needed on the direct and indirect effects aerosols have on cloud cover over cities.

8 | CONCLUSIONS

Previous research has shown an enhancement of cloud cover over urban areas. This study aimed to understand this cloud enhancement, specifically over London, UK using a mesoscale model. UK Met Office high-resolution regional forecasts are compared to observations, for the spring and summer period in 2014. First, the model simulations are analysed to establish if this cloud enhancement can be reproduced. The forecasts have systematic biases, with the modelled atmosphere not dry enough over the city, resulting in underestimated cloud-base heights. Despite this, the modelled cloud cover shows enhancement over the city compared to the rural surroundings, but the magnitude is underestimated. The largest modelled cloud cover enhancement over the city occurs during low wind speed conditions. A thermal circulation is found to be generated by the higher buoyancy flux over the city which can interact with a sea breeze. The circulation leads to horizontal moisture advection in the lowest 300 m of the atmosphere. The moisture convergence over the city transports the moisture upwards. In the upper part of the boundary layer, the turbulent moisture flux transports the moisture to the cloud layer.

The results are derived from analysis of 39 days, which provides confidence that processes will be similar in other cases. In the case of London, other mesoscale processes interact with city-scale processes, for example, the sea-breeze circulation. Therefore, studies in different geographical settings and climates are needed.

ACKNOWLEDGEMENTS

This research was funded by the NWO Rubicon grant "Clouds above the city" (019.161LW.026). S.G. is supported by the UK-China Research & Innovation Partnership Fund through the Met Office Climate Science for Service Partnership (CSSP) China as part of the Newton Fund. The authors thank Humphrey Lean for sorting logistics for system access.

AUTHOR CONTRIBUTIONS

Natalie E. Theeuwes: Conceptualization, Formal analysis, Methodology, Validation, Visualization, Writing-original draft, Writing-review & editing. **Ian A. Boutle:** conceptualization; validation; writing – original draft; writing – review and editing. **Peter A. Clark:** investigation; methodology; writing – review and editing. **Sue Grimmond:** data curation; project administration; writing – review and editing.

ORCID

Natalie E. Theeuwes https://orcid.org/0000-0002-9277-8551
Peter A. Clark https://orcid.org/0000-0003-1001-9226
Sue Grimmond https://orcid.org/0000-0002-3166-9415

REFERENCES

Ado, H.Y. (1992) Numerical study of the daytime urban effect and its interaction with the sea breeze. *Journal of Applied Meteorology*, 31, 1146–1164.

Angevine, W.M., White, A.B., Senff, C.J., Trainer, M., Banta, R.M. and Ayoub, M.A. (2003) Urban–rural contrasts in mixing height and cloudiness over Nashville in 1999. *Journal of Geophysical Research: Atmospheres*, 108.

Barlow, J.F., Halios, C.H., Lane, S. and Wood, C.R. (2015) Observations of urban boundary layer structure during a strong urban heat island event. *Environmental Fluid Mechanics*, 15, 373–398.

Best, M. (2005) Representing urban areas within operational numerical weather prediction models. *Boundary-Layer Meteorology*, 114, 91–109.

Best, M., Pryor, M., Clark, D., Rooney, G., Essery, R., Ménard, C., Edwards, J., Hendry, M., Porson, A. and Gedney, N. (2011) The Joint UK Land Environment Simulator (JULES), model description–Part 1: energy and water fluxes. *Geoscientific Model Development*, 4, 677–699.

Bornstein, R.D. and Johnson, D.S. (1977) Urban–rural wind velocity differences. *Atmospheric Environment (1967)*, 11, 597–604.

Bosman, P.J., van Heerwaarden, C.C. and Teuling, A.J. (2019) Sensible heating as a potential mechanism for enhanced cloud formation over temperate forest. *Quarterly Journal of the Royal Meteorological Society*, 145, 450–468.

Boutle, I.A., Finnenkoetter, A., Lock, A.P. and Wells, H. (2016) The London model: forecasting fog at 333 m resolution. *Quarterly Journal of the Royal Meteorological Society*, 142, 360–371.

Brown, A.R., Beare, R.J., Edwards, J.M., Lock, A.P., Keogh, S.J., Milton, S.F. and Walters, D.N. (2008) Upgrades to the boundary-layer scheme in the Met Office numerical weather prediction model. *Boundary-Layer Meteorology*, 128, 117–132.

Changnon, S.A.Jr., Huff, F.A. and Semonin, R.G. (1971) METROMEX: an investigation of inadvertent weather modification. *Bulletin of the American Meteorological Society*, 52, 958–968.

Christen, A. and Vogt, R. (2004) Energy and radiation balance of a central European city. *International Journal of Climatology*, 24, 1395–1421.

Clark, P.A., Harcourt, S.A., Macpherson, B., Mathison, C.T., Cusack, S. and Naylor, M. (2008) Prediction of visibility and aerosol within the operational Met Office Unified Model. I: model formulation and variational assimilation. *Quarterly Journal of the Royal Meteorological Society*, 134, 1801–1816.

Dou, J., Wang, Y., Bornstein, R. and Miao, S. (2015) Observed spatial characteristics of Beijing urban climate impacts on summer thunderstorms. *Journal of Applied Meteorology and Climatology*, 54, 94–105.

Drew, D.R., Barlow, J.F. and Lane, S.E. (2013) Observations of wind speed profiles over Greater London, UK, using a Doppler lidar. *Journal of Wind Engineering and Industrial Aerodynamics*, 121, 98–105.

Ek, M. and Mahrt, L. (1994) Daytime evolution of relative humidity at the boundary-layer top. *Monthly Weather Review*, 122, 2709–2721.

Findell, K.L. and Eltahir, E.A. (2003a) Atmospheric controls on soil moisture–boundary layer interactions. Part I: framework development. *Journal of Hydrometeorology*, 4, 552–569.

Findell, K.L. and Eltahir, E.A. (2003b) Atmospheric controls on soil moisture–boundary layer interactions. Part II: feedbacks within the continental United States. *Journal of Hydrometeorology*, 4, 570–583.

Grimmond, C.S.B. and Oke, T.R. (1995) Comparison of heat fluxes from summertime observations in the suburbs of four North American cities. *Journal of Applied Meteorology*, 34, 873–889.

Han, J.-Y. and Baik, J.-J. (2008) A theoretical and numerical study of urban heat island-induced circulation and convection. *Journal of the Atmospheric Sciences*, 65, 1859–1877.

Hertwig, D., Grimmond, C.S.B., Hendry, M.A., Saunders, B., Wang, Z., Jeoffrion, M., Vidale, P.L., McGuire, P.C., Bohnenstengel, S.I., Ward, H.C. and et al. (2020) Urban signals in high-resolution weather and climate simulations: role of urban land-surface characterisation. *Theoretical and Applied Climatology*, 142, 701–728.

Hidalgo, J., Pigeon, G. and Masson, V. (2008) Urban-breeze circulation during the CAPITOUL experiment: observational data analysis approach. *Meteorology and Atmospheric Physics*, 102, 223–241.

Hogan, R.J., O'Connor, E.J. and Illingworth, A.J. (2009) Verification of cloud-fraction forecasts. *Quarterly Journal of the Royal Meteorological Society*, 135, 1494–1511.

Illingworth, A.J., Hogan, R., O'Connor, E.J., Bouniol, D., Brooks, M.E., Delanoë, J., Donovan, D.P., Eastment, J.D., Gaussiat, N., Goddard, J.W.F., Haeffelin, M., Klein Baltink, H., Krasnov, O.A., Pelon, J., Piriou, J.-M., Protat, A., Russchenberg, H.W.J., Seifert, A., Tompkins, A.M., van Zadelhoff, G.-J., Vinit, F., Willén, U., Wilson, D.R. and Wrench, C.L. (2007) Cloudnet: continuous evaluation of cloud profiles in seven operational models using ground-based observations. *Bulletin of the American Meteorological Society*, 88, 883–898.

Kingfield, D.M., Calhoun, K.M., de Beurs, K.M. and Henebry, G.M. (2018) Effects of city size on thunderstorm evolution revealed through a multiradar climatology of the central United States. *Journal of Applied Meteorology and Climatology*, 57, 295–317.

Kotthaus, S. and Grimmond, C.S.B. (2014) Energy exchange in a dense urban environment–Part I: temporal variability of long-term observations in central London. *Urban Climate*, 10, 261–280.

Kotthaus, S. and Grimmond, C.S.B. (2018) Atmospheric boundary-layer characteristics from ceilometer measurements. Part 1: a new method to track mixed-layer height and classify clouds. *Quarterly Journal of the Royal Meteorological Society*, 144, 1525–1538.

Lawrence, M.G. (2005) The relationship between relative humidity and the dewpoint temperature in moist air: a simple conversion and applications. *Bulletin of the American Meteorological Society*, 86, 225–234.

Lemonsu, A. and Masson, V. (2002) Simulation of a summer urban breeze over Paris. *Boundary-Layer Meteorology*, 104, 463–490.

Li, Y., Fowler, H.J., Argüeso, D., Blenkinsop, S., Evans, J.P., Lenderink, G., Yan, X., Guerreiro, S.B., Lewis, E. and Li, X.-F. (2020) Strong intensification of hourly rainfall extremes by urbanization. *Geophysical Research Letters*, 47(14). https://doi.org/10.1029/2020GL088758

Liu, J. and Niyogi, D. (2019) Meta-analysis of urbanization impact on rainfall modification. *Scientific reports*, 9, 1–14.

Lock, A.P., Brown, A.R., Bush, M.R., Martin, G.M. and Smith, R.N.B. (2000) A new boundary-layer mixing scheme. Part I: scheme description and single-column model tests. *Monthly Weather Review*, 128, 3187–3199.

Omidvar, H., Bou-Zeid, E., Li, Q., Mellado, J.-P. and Klein, P. (2020) Plume or bubble? Mixed-convection flow regimes and city-scale circulations. *Journal of Fluid Mechanics*, 897, A5

Rosenfeld, D. (2000) Suppression of rain and snow by urban and industrial air pollution. *Science*, 287, 1793–1796.

Roth, M. (2000) Review of atmospheric turbulence over cities. *Quarterly Journal of the Royal Meteorological Society*, 126, 941–990.

Rozoff, C.M., Cotton, W.R. and Adegoke, J.O. (2003) Simulation of St. Louis, Missouri, land use impacts on thunderstorms. *Journal of Applied Meteorology*, 42, 716–738.

Schmid, P.E. and Niyogi, D. (2017) Modeling urban precipitation modification by spatially heterogeneous aerosols. *Journal of Applied Meteorology and Climatology*, 56, 2141–2153.

Smith, R.N.B. (1990) A scheme for predicting layer clouds and their water content in a general circulation model. *Quarterly Journal of the Royal Meteorological Society*, 116, 435–460.

Teuling, A.J., Taylor, C.M., Meirink, J.F., Melsen, L.A., Miralles, D.G., Van Heerwaarden, C.C., Vautard, R., Stegehuis, A.I., Nabuurs, G.-J. and de Arellano, J.V.-G. (2017) Observational evidence for cloud cover enhancement over western European forests. *Nature Communications*, 8. https://doi.org/10.1038/ncomms14065

Theeuwes, N.E., Barlow, J.F., Teuling, A.J., Grimmond, C.S.B. and Kotthaus, S. (2019) Persistent cloud cover over mega-cities linked to surface heat release. *npj Climate and Atmospheric Science*, 2, 15

Thielen, J., Wobrock, W., Gadian, A., Mestayer, P. and Creutin, J.-D. (2000) The possible influence of urban surfaces on rainfall development: a sensitivity study in 2D in the meso-γ-scale. *Atmospheric Research*, 54, 15–39.

Tripoli, G.J. and Cotton, W.R. (1980) A numerical investigation of several factors contributing to the observed variable intensity of deep convection over south Florida. *Journal of Applied Meteorology*, 19, 1037–1063.

van Heerwaarden, C.C., Guerau, V. and de Arellano, J. (2008) Relative humidity as an indicator for cloud formation over heterogeneous land surfaces. *Journal of the Atmospheric Sciences*, 65, 3263–3277.

Varentsov, M., Wouters, H., Platonov, V. and Konstantinov, P. (2018) Megacity-induced mesoclimatic effects in the lower atmosphere: a modeling study for multiple summers over Moscow, Russia. *Atmosphere*, 9, 50

Walters, D., Boutle, I.A., Brooks, M., Melvin, T., Stratton, R.A., Vosper, S.B., Wells, H., Williams, K., Wood, N., Allen, T., Bushell, A., Copsey, D., Earnshaw, P., Edwards, J., Gross, M., Hardiman, S., Harris, C., Heming, J., Klingaman, N., Levine, R., Manners, J., Martin, G., Milton, S.F., Mittermaier, M., Morcrette, C.J., Riddick, T., Roberts, M., Sanchez, C., Selwood, P., Stirling, A., Smith, C., Suri, D., Tennant, W., Vidale, P.L., Wilkinson, J., Willett, M., Woolnough, S. and Xavier, P. (2017). The Met Office Unified Model Global Atmosphere 6.0/6.1 and JULES Global Land 6.0/6.1 configurations. *Geoscientific Model Development*, 10(4), 1487–1520. http://dx.doi.org/10.5194/gmd-10-1487-2017.

Wang, W. (2009) The influence of thermally-induced mesoscale circulations on turbulence statistics over an idealized urban area under a zero background wind. *Boundary-Layer Meteorology*, 131, 403–423.

Warren, E., Charlton-Perez, C., Kotthaus, S., Lean, H.W., Ballard, S.P., Hopkin, E. and Grimmond, C.S.B. (2018) Evaluation of forward-modelled attenuated backscatter using an urban ceilometer network in London under clear-sky conditions. *Atmospheric Environment*, 191, 532–547.

Westra, D., Steeneveld, G. and Holtslag, A. (2012) Some observational evidence for dry soils supporting enhanced relative humidity at the convective boundary-layer top. *Journal of Hydrometeorology*, 13, 1347–1358.

Wilkinson, J.M., Porson, A.N.F., Bornemann, F.J., Weeks, M., Field, P.R. and Lock, A.P. (2013) Improved microphysical parametrization of drizzle and fog for operational forecasting using the Met Office Unified Model. *Quarterly Journal of the Royal Meteorological Society*, 139, 488–500.

Zhong, S., Qian, Y., Zhao, C., Leung, R. and Yang, X.-Q. (2015) A case study of urbanization impact on summer precipitation in the Greater Beijing Metropolitan Area: urban heat island versus aerosol effects. *Journal of Geophysical Research: Atmospheres*, 120, 10903–10914.

Zhu, X., Li, D., Zhou, W., Ni, G., Cong, Z. and Sun, T. (2017) An idealized LES study of urban modification of moist convection. *Quarterly Journal of the Royal Meteorological Society*, 143, 3228–3243.

How to cite this article: Theeuwes, N.E., Boutle, I.A., Clark, P.A. & Grimmond, S. (2021) Understanding London's summertime cloud cover. *Quarterly Journal of the Royal Meteorological Society*, 1–12. Available from: https://doi.org/10.1002/qj.4214